MISALIGNMENT STUDIES OF LCLS-II SC LINAC*

A. Saini†, N. Solyak, V. Yakovlev, FNAL, Batavia, IL 60510, USA
T. Raubenheimer, SLAC, Stanford, CA 94309, USA

Abstract

The Linac Coherent Light Source (LCLS) is an x-ray free electron laser facility. The proposed upgrade of the LCLS facility is based on construction of a 4 GeV superconducting (SC) linear accelerator (linac). An optimal reliable performance of the linac is largely determined by beam sensitivity to various component alignment errors. In this paper we evaluate misalignment tolerances of the LCLS-II SC linac using a more realistic alignment model that includes correlated misalignment of elements.

INTRODUCTION

The Linac Coherent Light Source -II (LCLS–II) is a proposed fourth generation x-ray light source facility [1]. It is based on a 4 GeV superconducting radio frequency (SCRF) linear accelerator that would operate in continuous wave (CW) regime. Operational goal of the LCLS-II project is to provide a high brightness x-ray source for broad-range of applications. This could only be achieved if SC linac would succeed to deliver a high quality ultra-low emittance beam to the undulator. Thus, one of the primary accelerator design and operational objectives for the LCLS-II linac is the preservation of beam emittances during acceleration and beam manipulation. The principal sources of emittance dilution in the linac are dispersion resulting from misaligned quadrupoles, pitched cavities, wake fields generated from the cavity offsets, coupling between transverse planes due to quadrupole roll errors (rotation of polls of quadrupole magnets) and cryomodule offsets. This, in turn requires stringent tolerances on the alignment of beam-line elements. A study had been performed for the LCLS-II SC linac using a set of alignment tolerances and emittance dilution under those tolerances was reported elsewhere [2]. However, in this study we considered random uncorrelated misalignments of the beam-line elements; each element was misaligned independently to each other. However, different stages of assembly and commissioning introduce a sort of correlated misalignments among the elements in the beam line. The correlated misalignment introduces a common offset to the group of elements. Consequently, it results in coherent kicks to the beam centroid from misaligned elements and therefore, its impact is more severe than uncorrelated misalignments that offer a random kick to the beam centroid. In this paper we present correlated misalignments budget for the LCLS-II SC linac and evaluate emittance dilution with these errors using a more realistic model that includes correlated misalignments at different stages of the linac commissioning. Furthermore, emittance compensation using one to one steering orbit correction algorithm is also discussed.

* Work supported in part by Fermi Research Alliance, LLC under USA DOE Contract No. DE-AC02-07CH11359, DOE Contract No. DE-AC02-76SF00515 and the LCLS-II Project.
† asaini@fnal.gov

LCLS-II SC LINAC

The SC linac is segment into five sections which are named as L0, L1, HL, L2 and L3. All the sections except L1 and HL are separated to each other by intermediate warm sections which are designed for the specific purposes such as laser heating, diagnostic and bunch compressions.

Excluding HL, all sections are composed of 9-cell 1.3 GHz SC TESLA like cavities [3]. HL section consists of 9-cell, 3.9 GHz SC cavities [4]. Number of elements and their nominal operational RF parameters in each section are summarized in Table 1. It should be noted that linac design is continuously evolving in order to address the beam optics and the technological constraints and therefore, configuration of the linac presented here may differ from the design presented elsewhere [5]. However, outcomes of this study are still valid and directly applicable to the LCLS-II SC linac.

Table 1: Configuration of each Section in LCLS-II Linac

	Phase (deg)	Gradient (MV/m)	No. of CM's	Avail. cavities	Energy (MeV)
L0	~0	15.96	1	8	0.75-98
L1	-21.0	13.23	2	16	98-303
HL	-165	13.25	2	16	303-250
L2	-21	14.52	12	96	250-1600
L3	0	14.46	20	144	1600-4000

SOURCES OF MISALIGNMENTS

Figure 1 shows a schematic of 1.3 GHz cryomodule (CM). It accommodates eight 1.3 GHz cavities and a superconducting quadrupole magnet. The total length of CM is about 12.3 m. In this section we discuss the correlated misalignments introduced among the elements during a cryomodule assembly and linac commissioning.

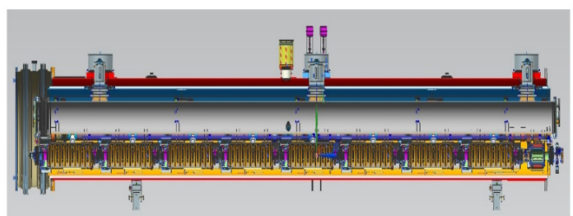

Figure 1: A lateral view of 1.3 GHz CM for LCLS-II linac.

Eight cavities are mounted on a string. During the assembly, each cavity is aligned with respect to the string-axis within an RMS transverse offset of 75μm. It can be observed from Figure 1 that 1.3 GHz CM consists of three cold mass supports. One at the middle is fixed while remaining at both ends are sliding cold mass supports. During CM transportation those sliding supports provide a

ISBN 978-3-95450-147-2

flexibility of lateral movement and therefore, reduce the impact of external force-impulses. However, a misalignment budget of 0.3mm RMS transverse offset of string with respect to CM axis is allotted during CM transportation. This offset is distributed with the repeating scale of 3m. Thus, it introduces a correlated misalignment among the elements situated on this scale. All CMs are cooled down from room temperature to operating temperature (2K) during the linac commissioning. This process results in the shrinkage of element's surface and therefore results in a transverse misalignment of the string w.r.t. CM axis. An alignment tolerance of RMS 0.175 mm is assigned for warm to cold transition of the CM and it is also distributed with 3m repeating pattern. Cryomodules are aligned in a tunnel w.r.t the reference network line within an RMS tolerance of 50μm.

Network Line Misalignment

A set of reference markers is positioned along the beam line. Coordinates of those markers are measured using GPS technique. Thus, a set of primary reference points is established. Collection of those reference points along the beam line makes a network line (also called survey line). Because of the narrow tunnel, refraction will affect measurements and therefore, survey process may have an error that leads to deviation of the network line from its true position. The network line misalignment propagates as a wave [6]. Its amplitude and wavelength assigned for the LCLS-II tunnel are 0.3mm and 100m respectively. As all CMs are aligned w.r.t. the network line therefore, a misalignment in network line is eventually translated to the CM offset (Δy) and its magnitude is estimated using following equation:

$$\Delta y = A\sin\left(\frac{2\pi}{\lambda}z_{cm} + \varphi\right); \qquad (1)$$

where A is amplitude, λ is wavelength, z_{cm} is central position of CM in beamline and ϕ is arbitrary phase of the wave. Figure 2 shows a distribution of network line offsets along L2 section in the LCLS-II SC linac. It can be observed that resulting CMs offsets depend on their locations in the beamline. A summary of misalignment errors and their magnitudes for the LCS-II SC linac are shown in Table 2.

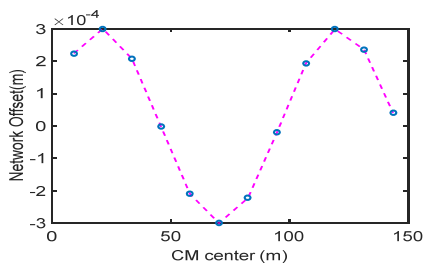

Figure 2: Propagation of a network line misalignment (magenta line) along L2 section of the linac. Resulting CM offsets are shown using blue dots.

Table 2: Alignment Tolerances for LCLS-II SC Linac [6]

Source	Amplitude	Scale
Elements on string	75 μm	-
CM Transportation	0.3 mm	3 m
Warm to Cold Transition	0.175 mm	3 m
CM in Tunnel	50 μm	13 m
Network	0.3 mm	100 m

Model Implementation

With the intent of a realistic estimation of misalignment tolerances of the LCLS-II SC linac, a model is implemented in Matlab and interfaced with the beam-dynamics code LUCRETIA [7]. The correlated misalignment model makes possible to apply several layers of the misalignment errors simultaneously. First, elements are misaligned randomly on a string and then string misalignment w.r.t. CM axis is applied. String RMS pitch angle (θ_s^{RMS}) is determined from its RMS offset (Δx_s^{RMS}) using following equation:

$$\tan(\theta_s^{RMS}) = \left(\frac{2\Delta x_s^{RMS}}{L_s}\right) \qquad (2)$$

where L_s is length of a string. All strings are misaligned randomly with given RMS offset and RMS pitched angle. Resulting offset (Δx^i) of the i^{th} element situated on a misaligned string is obtained using following equation:

$$\Delta x^i = S * \tan(\theta_s) + \Delta x_s \qquad (3)$$

where S is distance of the element center from the string center, Δx_s and θ_s are offset and pitch angle of the string respectively. First term in equation (3) corresponds to the element offset introduced by a pitch error.

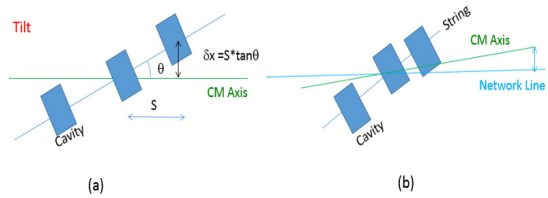

Figure 3: A schematic of (a) String pitch misalignment w.r.t. CM axis; (b) CM misalignment w.r.t. network line.

Using same approach CM misalignments w.r.t network line and network line errors w.r.t. ideal survey line are translated to the individual element's offset. Total offset of the i^{th} element after applying all misalignment errors is:

$$\Delta x^i{}_{total} = \Delta x^i{}_{ind} + (\Delta x + \delta x)_s + (\Delta x + \delta x)_{CM} + (\Delta x + \delta x)_{NE}; \qquad (4)$$

where Δx^i_{ind} is an uncorrelated misalignment of the i^{th} element, δx is the element offset due to the pitch error, subscripts *s, CM* and *NE* correspond to string, CM and network line errors respectively.

MISALIGNMENT STUDIES

Two major sections of the LCLS-II SC linac are L2 and L3, which are composed of 12 and 20 CMs respectively. Thus, study is performed to understand implications of correlated misalignments in both sections using a beam dynamics code LUCRETIA. Misalignment tolerances

specified in Table 2 are applied in the vertical plane and simulation is performed using a Gaussian distribution of 50k macro particles corresponding to the bunch charge of 300pC. Effects of the initial beam offset and the short-range wake fields are also included.

Misalignment Studies in L2 Section

RMS bunch length and relative energy spread at the beginning of L2 section are 0.28 mm and 1.31 % respectively. Initial normalized RMS beam emittance is 0.45 mm-mrad in both horizontal and vertical planes. Figure 4 shows distribution of emittance dilution of all machines. It can be noticed that resulting emittance dilution in some machines are as large as 0.8 mm-mrad. However 90 % and mean emittance dilution are 0.16 and 0.36 mm-mrad respectively. One to One steering algorithm is applied to correct beam trajectory and thus, to compensate emittance dilution.

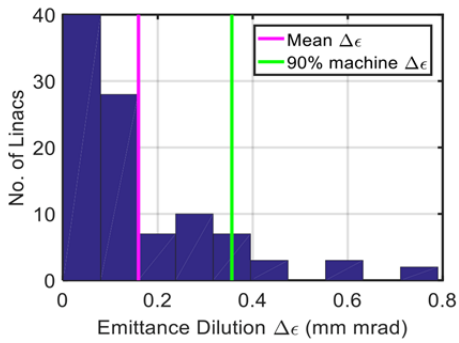

Figure 4: Resulting emittance growth distribution in L2 section for 100 machines. 90% and mean emittance growth are shown in green and magenta respectively.

It can be observed from left plot in Figure 5 that in some cases maximum excursion of vertical beam centroid without correction is around 5mm. The golden beam centroid trajectories (that include BPMs offsets and vertical beam centroid positions) after applying corrections are shown by green lines in the plot. It can be noticed that centroid golden trajectories are confined within 1mm. Mean emittance growth along the L2 section is shown on the right plot in Figure 5. It can be observed that final emittance growth is reduced from 0.61 to 0.47 mm-mrad after applying one to one correction scheme.

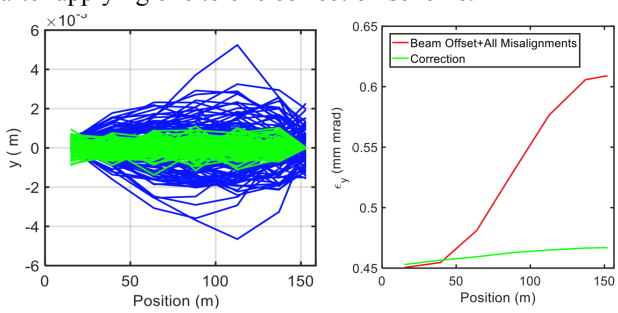

Figure 5: (Left) Beam centroid trajectories before (blue) and after (green) one to one correction in L2 section for 100 machines. (Right) Mean emittance evolution without (red) and with (green) correction along L2 section.

Misalignment Studies in L3 Section

RMS bunch length and energy spread used at the beginning of L3 section are 0.044 mm and 0.439 % respectively. Initial normalized rms emittances are same as used in L2 section.

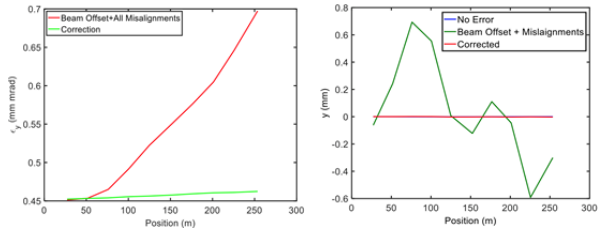

(a) (b)

Figure 6: (a) Mean emittance (b) mean vertical centroid trajectories along L3 section.

Similar study was performed for the L3 section. Figure 6(a) shows mean emittance evolution without correction (red line) and with correction (green line). It can be observed that after applying one to one steering mean final emittance at the end of L3 section is restored from 0.7 to 0.46 mm-mrad. Figure 6(b) shows mean vertical beam centroid trajectory for different cases along the L3 section.

CONCLUSION

A model is implement to study implications of correlated misalignment in the LCLS-II SC linac. Resulting emittance growth is larger than uncorrelated misalignments. However, one to one steering algorithm effectively compensate the emittance growth and restored it within 4% and 3% for L2 and L3 sections respectively.

ACKNOWLEDGMENT

Author would like to thank George Gassner, Tug Arkan and Virgil Bocean for useful discussion about alignment tolerances and Glen White for useful discussion about Lucretia.

REFERENCES

[1] T.O. Raubenheimer, “LCLS-II: Status of the CW X-ray FEL Update to the LCLS Facility,” FEL’15, Daejeon, Korea (2015).

[2] A. Saini *et al.*, “Study of Beam-Based Alignment for the LCLS-II SC Linac,” LINAC’14, Geneva (2014).

[3] Aune B *et al.*, 2000 Superconducting TESLA cavities Phys.Rev. ST Accel. Beams 3 092001-1-25.

[4] E. Harms *et al.*, “Status of 3.9 GHz Superconducting RF cavity technology at Fermilab,” THP028, LINAC’08, British Columbia, Canada (2008).

[5] P. Emma *et al.*, “Linear Accelerator Design for the LCLS-II FEL facility,” FEL’14, Basel (2014).

[6] G. Gassner, “LCLS-II Cryomodule Alignment,” LCLS-II Accelerator Physics Meetings.

[7] `http://www.slac.stanford.edu/accel/ilc/codes/Lucretia/.`

ISBN 978-3-95450-147-2